



## Research Article

# EVALUATION OF DIFFERENT COMPUTER CODES FOR GENERATION OF X-RAY SPECTRA IN GENERAL DIAGNOSTIC RADIOGRAPHY

*Bui Ngoc Huy\**, *Pham Van Dung*

*Dalat Nuclear Research Institute, Vietnam*

*\*Corresponding author: Bui Ngoc Huy –Email: [huyngoc192@yandex.ru](mailto:huyngoc192@yandex.ru)*

*Received: September 18, 2023; Revised: October 30, 2023; Accepted: November 13, 2023*

## ABSTRACT

*This study presents the simulation results of the X-ray spectra of the general diagnostic radiography unit by using an empirical model (Spektr 3.0), semi-empirical models (IPEM 78 report No.78, SpekPy, and Xpecgen), and a Monte Carlo model (EGSnrc). The general diagnostic machine was assessed by quality assurance testing. The half-value layer (HVL), mean energy ( $E_{mean}$ ), and Air kerma per milliampere-second ( $K_{air}/mAs$ ) have been measured at different tube voltages and compared with those obtained from five computer codes. The heel effect and target material composition were investigated. The IPEM report No.78 was used as a reference to compare with other computer codes. The comparative assessment showed that the HVL,  $E_{mean}$ , and  $K_{air}/mAs$  were well-matched between the five codes and physical measurements in diagnostic radiology energy ranges. The Monte Carlo modeling is a sophisticated, precise computational tool that can characterize the spectra of newly developed target material compositions, complex geometrical configurations, and contributions of secondary particles, which are mostly empirical and semi-empirical models that currently can't be performed accurately.*

**Keywords:** EGSnrc simulation; Half-value layer; Monte Carlo; Radiography; X-ray spectra

## 1. Introduction

General radiography is an important, quick, and painless diagnostic tool in medical imaging to spot problems in the body's internal structures. X-ray machine is widely used in hospitals and clinics and has become an indispensable medical diagnostic method. We now have a better understanding of the risks associated with X-ray radiation and have developed protocols to minimize unnecessary radiation exposure dose and improve image quality.

The spectrum of diagnostic X-rays cannot be measured precisely, and thus other methods of predicting X-ray spectra have been developed to generate X-ray spectra from tungsten targets. These methods are divided into three categories: empirical (Archer & Wagner, 1988; Boone et al., 1997; Boone & Seibert, 1997; Fewell & Shuping, 1977; Waggener et al., 1999), semi-empirical models (Birch & Marshall, 1979; Blough et al., 1998;

---

*Cite this article as:* Bui, N. H., & Pham, V. D (2025). Evaluation of different computer codes for generation of X-ray spectra in general diagnostic radiography. *Ho Chi Minh City University of Education Journal of Science*, 22(3), 475-486. [https://doi.org/10.54607/hcmue.js.22.3.3967\(2025\)](https://doi.org/10.54607/hcmue.js.22.3.3967(2025))

Iles, 1987; Tucker et al., 1991), and Monte Carlo (MC) simulations (Ay et al., 2004; Kawrakow, 2000; Kulkarni & Supe, 1984; Ng, Kwok & Tang, 2000; Taleei & Shahriari, 2009). MC simulation uses the direct transport of electrons and generated photons in the target and filter for the calculation of X-ray spectra. MC simulation is a powerful tool that offers several advantages by providing detailed information about the interactions in complex geometries. Even when tube voltage and target angle are constant, the predicted spectra do not share the same X-ray energy distribution and intensity. Therefore, it is necessary to assess the accuracy of predicted spectra using these methods and their possible effect on the performance parameters of medical imaging systems and radiation dosimetry calculations.

In this study, the IPEM report No.78 [Institute of Physics and Engineering in Medicine (IPEM)] (Morrison, 1998) was used as a reference to compare with other computer codes in diagnostic radiography energy ranges (at 70, 80, and 90 kVp). The HVL,  $E_{\text{mean}}$ , and  $K_{\text{air}}/\text{mAs}$  have been measured and compared with those from the simulation. In addition, the anode heel effect and target material composition were evaluated. The HVL,  $E_{\text{mean}}$ , spectra, and  $K_{\text{air}}/\text{mAs}$  were caused by five computer codes, and the measurements showed that all have good agreement with the IPEM report No.78 and International Electrotechnical Commission (IEC) 60601-1-3 requirements (Hyemin et al., 2018).

## 2. Materials and methods

### 2.1. Computer codes

IPEM report No.78 - a software provides X-ray spectra from a tungsten target with an anode angle of 6-22 degrees at tube voltages ranging 30-150kV and spectra from molybdenum and rhodium with an anode angle of 9-23 degrees at tube voltages ranging 25-32kV. The additional filter can be made out of various materials, energy bin in all spectra was provided 0.5 keV. The model was developed by Birch and Marshall and includes an empirical function for the bremsstrahlung cross-section differential in photon energy, integrated over the electron energy based on the Bethe stopping power formula (Bethe, 1930). The model approximates the depth of bremsstrahlung production using the Thomson–Whiddington relation (Whiddington, 1912), which relates the electron energy loss to the penetration depth. Due to its popularity and widespread availability in the radiological physics field, the IPEM report No.78 was used as a reference to compare with other computational codes.

Spektr 3.0 (Punnoose et al., 2016) - a MATLAB (Matlab, 2023) toolkit for calculation of X-ray spectra, beam quality, HVL,  $K_{\text{air}}$ , and fluence per unit exposure from 1keV to 150keV in 1keV energy bins using a tungsten anode spectral model using the interpolating cubic splines (TASMICS) algorithm (Hernández & Boone, 2014) at 100cm from the focal spot. TASMICS uses piecewise third-order polynomial spline approximations analogous to computing the number of photons in each energy bin as a function of tube voltages. For the high-energy bins, Spektr 3.0 produces a more accurate polynomial fitting to approximate the photon fluence. The main modules of this toolkit are: *spektr.m* - start graphical user interface, *Spektr*, *spektrAirKerma.m* - calculate  $K_{\text{air}}$  for the inputted spectrum,

*spektrFluencePerAirKerma.m* - generates the fluence per Air Kerma, *spektrExposure.m* generates the exposure, *spektrHVLn.m* - calculates the n'th HVL (n - number of the HVL to calculate), *spektrMeanEnergy.m* - function returns the  $E_{\text{mean}}$  of the X-ray spectra, *spektrSpectrum.m* - function will generate an X-ray spectrum at the specified potential (of the generator) that is set to a constant 1mAs.

SpekPy - a Python programming language toolkit to generate X-ray spectra from tungsten, molybdenum, and rhodium targets (Bujila et al., 2020). SpekPy utilizes the photon cross-sections (for both mass attenuation and mass energy absorption) derived from the PENELOPE code system (Salvat et al., 2006) to filter spectra and calculate HVL, photon energies of X-rays. These cross-sections were also used for the calculation of the HVLs from the National Institute of Standards and Technology (NIST) dataset. The fluence,  $K_{\text{air}}$ ,  $E_{\text{mean}}$ ,  $E_{\text{effective}}$ , first and second HVL values (in mmAl and mmCu), and homogeneity coefficient can be calculated from the spectrum. The keywords arguments in SpekPy were targ = W (anode material), kvp = 70/80/90 (tube voltages in kV), th = 16 (anode angle in degree), dk = 0.5 (bin width in keV), physics = "default" (name of the physics mode), mu data source = "pene" (linear attenuation data), char = True (whether the characteristic portion of spectrum is retained), Brem = "True" (whether the bremsstrahlung portion of spectrum is retained), mas = 1 (The exposure setting for the file spectrum), z,x,y = 75, -5, 5 (point of interest in cm), and obli = True (whether path-length through extrinsic filtration varies with x, y). SpekPy can also create a new material filter using weights with keywords: material density ( $\text{g/cm}^3$ ) and material composition (atomic number, weight). In this study, SpekPy was used for evaluating the anode heel effect at 90kVp with and without aluminium filters.

Xpccgen - a Python programming language package to calculate X-ray spectra generated in tungsten anode using the model from (Hernández & Fernández, 2016) at 100cm from the focal spot. The parameters used for calculation are given:  $E_0 = 70/80/90$  (electron kinetic energy in keV), theta = 16 (X-ray emission angle in degrees, e min = 3 (minimum kinetic energy to calculate in the spectrum in keV), num e = 120 (number of points to calculate in the spectrum), epsrel = 0.5 (the tolerance parameter used in numeric integration).

EGSnrc - Electron Gamma Shower from National Research Council Canada (Kawrakow, 2000) - a software toolkit released in 2020, utilities to build MC simulation of ionizing radiation transport (photons, electrons, positrons) through matter and complex geometries with energies from 1keV to 10GeV. In this study, the simulations were divided into two steps using the software included in the default installation package of EGSnrc. First, the X-ray machine was simulated using the BEAMnrc (Rogers et al., 2009) to obtain the spectrum at three kVps. A geometric schematic of the X-ray tube and collimator for EGSnrc simulation was shown in Figure 1 (not to scale).

The simulations were performed using Ncase = 1E8 histories, which was enough to achieve statistical accuracy. Electron and photon energy cut-offs were set to 0.512MeV and 0.001MeV, respectively. A pencil electron beam with a radius of 0.13 cm was used, incident laterally, with ISOURC = 10. The .pegs4dat file that contains cross-section information of all needed media can be generated by using egs\_gui. The phase-space files were calculated at a distance of 75cm from the center of the target.

The HVL,  $E_{mean}$ , and spectra of each kVp were obtained using egs\_cavity (Townson et al., 2020). The phase-space files obtained from BEAMnrc were used as input to run the egs\_cavity user code.

The calculations were performed using Ncase = 1E6 histories, photon splitting = 1000, electron and photon energy cut-off: 0.512MeV and 0.001MeV. The energy bin interval is 0.5keV. The HVL values were obtained by using the two-point method (Yagi et al., 2003). Table 1 shows the materials and inputs used to simulate this model. Table 2 shows a summary of the computer codes used for the generation of X-ray spectra.

**Table 1.** Materials and density in g/cm<sup>3</sup> of EGSnrc MC simulation

Material	Element	Density, g/cm <sup>3</sup>
Anode	90% W/10% Re	19.427
Pyrex glass	B, O, Na, Al, Si, K	2.23
Air	C, N, O, Ar	1.2048×10 <sup>-3</sup>
Lead shielding/ collimator shutters	Pb	11.35
Filter	Al	2.7
Anode axis	Mo	10.28

**Table 2.** Summary of computer codes used for the generation of X-ray spectra

Computer codes	Catalogy	Models used	Electron model	Bremsstrahlung model	Focal to Detector distance, cm
EGSnrc	MC simulation	MC	PRESTA-II	NIST data	75
SpekPy	Semi-empirical	SpekCalc	Diffusion approximation	UNI	75
Xpecgen	Semi-empirical	Birch and Marshall model (target pure W)	Explicit	UNI	100
Spektr 3.0	Empirical	TASMICS model	MCNPX	MCNPX	100
IPEM report No.78	Semi-empirical	Birch and Marshall model (90/10 W/Re)	Thomson-Whiddington	UNI	75

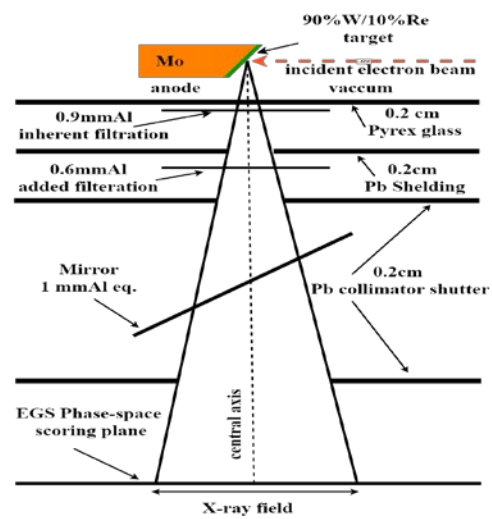


**Figure 1.** Geometric schematic of the X-ray tube and collimator for EGSnrc simulation

All simulations were performed on a computer with an Intel Core i5-4200U CPU 1.60GHz. The time of each simulation was from about a minute to seven hours. All output data files obtained from those computer codes were summarized, analyzed, and plotted in Mathematica software (Wolfram Mathematica, 2023).

The measurements and simulations were performed with a TXR full wave radiography X-ray machine, equipped with a Toshiba E7239GX tube (serial number: 14C413), marketed in 2014. The tube features a 74 mm anode with a target angle of 16 degrees. The target was built as rhenium-tungsten (90%W/10%Re) faced molybdenum, and 2.5mmAl equivalent filter (inherent filtration of 0.9mmAl and an additional filter of 1.6mmAl). The target was encased in a vacuum with 2.0mm-thick Pyrex glass. The X-ray tube housing contains 20 mm-thick lead shielding. A collimator is located beneath the tube, equipped with four 2.0 mm-thick lead shutters and a light and mirror system (1 mm Al equivalent) used to determine the light and radiation fields. The voltage ripple is less than 2%; however, it was not considered in the simulation.

## **2.2. Quality assurance (QA) using a non-invasive Accu-Gold+ Touch Pro diagnostic X-ray system**

The X-ray general diagnostics machine was assessed by testing parameters like reproducibility of kVp, dose output, and time exposure; accuracy of kVp, time exposure, mAs linearity, and HVL. All tested parameters must be matched to the national or/and international tolerance limits.

The physical measurements were performed using a calibrated Accu-Gold+ Touch Pro (AGT-P-AG, serial number 55-2036) with solid-state Accu-Gold Multi-Sensor (AGMS-DM, serial number 431483). AGMS-DM sensor enables the measurement of dose, dose/mAs, dose/pulse, dose rate, HVL, kVp, exposure time, pulse count with kVp ranging 20-160 (uncertainty 2%), exposure time ranging 1ms-300s (uncertainty 0.1%), HVL ranging 0.16-13.5mmAl with W anode (uncertainty 10%), and dose rate ranging 80nGy-100Gy (uncertainty 5%). Routine calibration of the QA system is required annually, traceable to the Secondary Standard Dosimetry Laboratory, Institute for Nuclear Science and Technology, Vietnam. The sensor was placed 75cm from the focal spot, radiation field of 10×10 cm<sup>2</sup>.

The QA test was taken three times for each kVp. For estimation  $E_{\text{mean}}$ , the mass attenuation coefficients ( $\mu/\rho$ ) were calculated from physical measurements of HVL by using the equation:  $\mu = \ln 2/\text{HVL}$  and aluminium density  $\rho = 2.7\text{g}/\text{cm}^3$ . The NIST data table (National Institute of Standards and Technology, 2004) was used for extrapolation of deposition X-ray energy by using the NonlinearModelFit model of Mathematica to link the points, then the  $E_{\text{mean}}$  was evaluated from the fitted function at each HVL value. The Plot function was used to visualize the fitted function with the data.

## **3. Results and discussion**

### **3.1. Results**

The study of QA consists of reproducibility of kVp, radiation output, and time exposure; accuracy of kVp and time exposure; mAs linearity, and HVL (Table 3). The

comparisons of simulated X-ray spectra for various tube voltages are shown in Figures 2, 3, and 4. The comparisons of HVL,  $E_{\text{mean}}$ ,  $K_{\text{air}}/\text{mAs}$ , and K-peaks energies are shown in Tables 4, 5, 6, and 7. The anode heel effects are shown in Figures 5 and 6. The assessment of various target compositions is illustrated in Figure 7. The fitted function used to estimate  $E_{\text{mean}}$  from physical measurements of the HVL is shown in Figure 8. The coefficient of linearity (CoL) is shown in Figure 9.

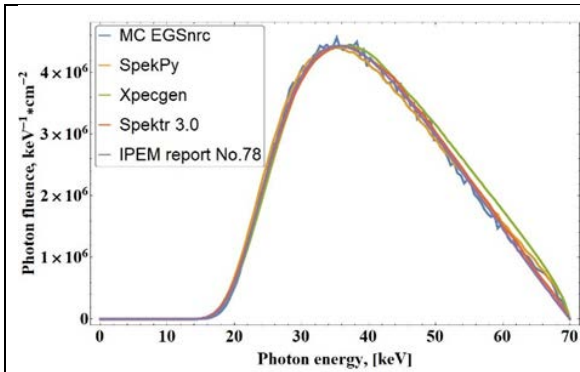


Figure 2. Comparison of the simulated X-ray spectra for 70kVp produced by five computer codes

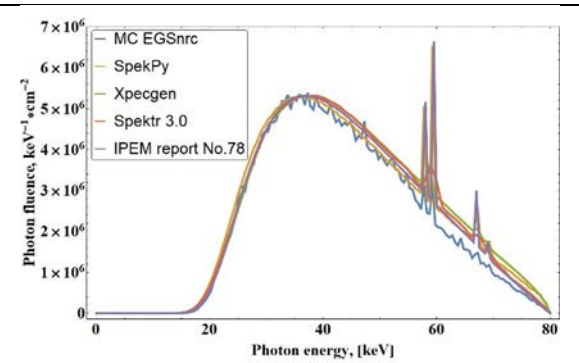


Figure 3. Comparison of the simulated X-ray spectra for 80kVp produced by five computer codes

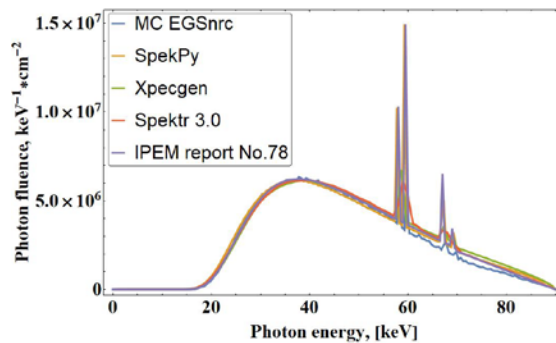


Figure 4. Comparison of the simulated X-ray spectra for 90kVp produced by five computer codes

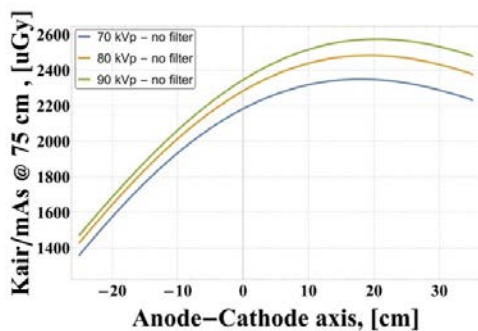


Figure 5. SpekPy simulated the heel effects for an anode without an aluminium filter at tube voltages of 70, 80, and 90kVp

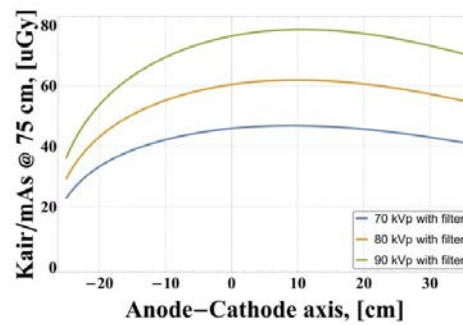


Figure 6. SpekPy simulated the heel effects for an anode with an aluminium filter at tube voltages of 70, 80, and 90kVp

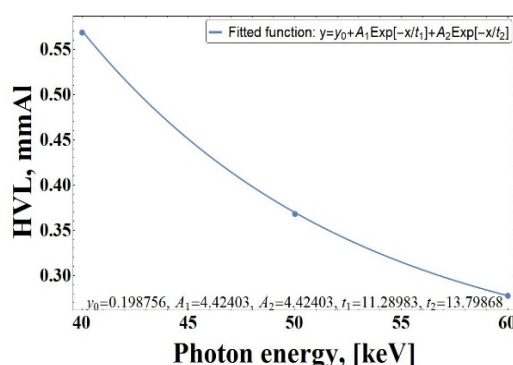
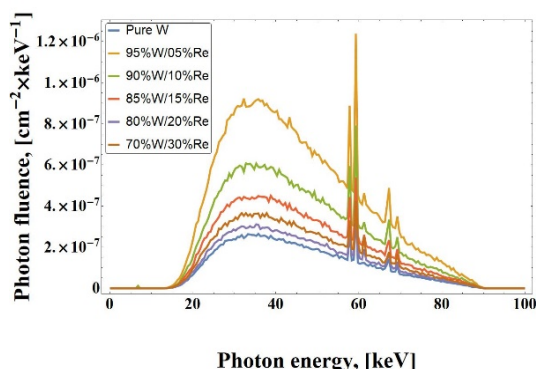


Figure 7. EGSnrc MC simulated spectra for various target compositions at tube voltage 90kVp

Figure 8. The fitted function was used to estimate  $E_{mean}$  from physical measurements of the HVL

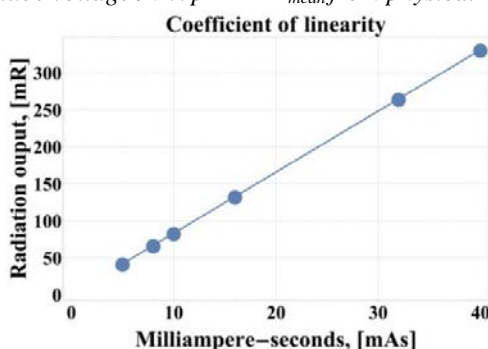


Figure 9. CoL calculated at 70kVp

Table 3. Results of QA tests for the general diagnostic X-ray machine

No	Parameters	Selected kVp	Tolerance, %	Baseline	Status
1	kVp accuracy	70	-1.29	less than -10% or less than -10 kV	pass
		80	-0.54		pass
		90	0.90		pass
2	kVp reproducibility	70	0.00	less than -5%	pass
		80	0.04		pass
		90	0.07		pass
3	Exposure time reproducibility	70	0.00	less than -10%	pass
		80	0.07		pass
		90	0.07		pass
4	Exposure time accuracy	70	-0.47	less than -20 % for times <100 ms	pass
		80	-0.54		pass
		90	-0.44		pass
5	Reproducibility of radiation output	70	0.11	less than -5%	pass
		80	0.09		pass
		90	0.07		pass
6	Coefficient of linearity	70	0.01	less than 0.1	pass
7	Radiation output linearity	70	1.44	less than -20%	pass

**Table 4.** Evaluation of five computer codes for HVL estimations for various tube voltages

Computer codes	70 kVp		80 kVp		90 kVp	
	HVL, mmAl	Diff, %	HVL, mmAl	Diff, %	HVL, mmAl	Diff, %
IPEM report No.78	2.84	-	3.25	-	3.68	-
Spektr 3.0	2.93	3.34	3.33	2.58	3.73	1.50
SpekPy	2.80	1.16	3.18	2.18	3.57	3.13
Xpecgen	2.90	2.13	3.28	0.86	3.67	0.11
EGSnrc MC	2.94	3.71	3.37	3.61	3.76	2.30
Measured	2.88	1.50	3.27	0.64	3.62	1.62
IEC 60601-1-3	>2.5	-	>2.9	-	>3.2	-

**Table 5.** Comparison of the  $E_{mean}$  at various tube voltages

Computer codes	70 kVp		80 kVp		90 kVp	
	$E_{mean}$ , keV	Diff, %	$E_{mean}$ , keV	Diff, %	$E_{mean}$ , keV	Diff, %
IPEM report No.78	40.80	-	44.50	-	47.80	-
Spektr 3.0	40.99	0.47	44.53	0.07	47.76	0.08
SpekPy	40.90	0.24	44.46	0.09	47.73	0.16
Xpecgen	42.98	5.21	47.05	5.56	50.89	6.27
EGSnrc MC	38.54	5.69	42.05	5.66	44.57	7.00
Measured	44.62	8.95	47.39	6.29	48.47	1.40

**Table 6.** Comparison of  $K_{air}$ /mAs (at 100 cm for Spektr 3.0 and Xpecgen codes)

Computer codes	70 kVp		80 kVp		90 kVp	
	$K_{air}$ /mAs, Gy	Diff, %	$K_{air}$ /mAs, Gy	Diff, %	$K_{air}$ /mAs, Gy	Diff, %
IPEM report No.78	101.60	-	132.90	-	167.00	-
Spektr 3.0	51.86	8.12	70.67	5.62	98.73	4.97
SpekPy	104.28	2.6	135.23	1.74	163.03	2.40
Xpecgen	51.71	8.41	69.69	7.01	97.77	7.84
EGSnrc MC	98.76	2.83	130.32	1.96	163.12	2.35
Measured	95.40	6.29	122.74	7.95	155.15	7.36

**Table 7.** Evaluation of X-ray characteristics K-peaks at 80 and 90kVp

kVp	K-peaks	Literature	IPEM report	Spektr 3.0	SpekPy	Xpecgen	EGSnrc MC
			No.78	Peak, keV	Peak, keV	Peak, keV	Peak, keV
80	$K_{\alpha 2}$	57.98	58	-	57.75	-	57.75
	$K_{\alpha 1}$	59.32	59.5	59	59.25	58.72	59.25
	$K_{\beta 1}$	67.24	67	67	67.25	67.23	64.25
	$K_{\beta 2}$	69.10	69	-	69.25	-	67.25
90	$K_{\alpha 2}$	57.98	58	-	57.75	-	58.25
	$K_{\alpha 1}$	59.32	59.5	59	59.25	58.54	59.75
	$K_{\beta 1}$	67.24	67	67	67.25	67.27	67.75
	$K_{\beta 2}$	69.10	69	-	69.25	-	69.75

**Table 8.** Differences in  $K_{air}$ /mAs at 100cm from the focal spot obtained by SpekPy at various kVp

kVp	Difference in $K_{air}$ /mAs, %	
	with an aluminium filter	without an aluminium filter
70	39.46	31.31
80	40.72	33.77
90	41.75	35.96

### 3.2. Discussion

#### 3.2.1. QA study

The QA assessment of the X-ray machine demonstrated satisfactory performance across all evaluated parameters, falling within the acceptable limits outlined in International Atomic Energy Agency (2023) and Shaw et al. (2020). As shown in Table 3, the accuracy of kVp gave a maximum %error of less than -1.29%, which is well below the threshold of -10%. Maximum exposure time accuracy was -0.54%, also below the allowable limit of -20% for exposure times under 100 ms. The reproducibility of kVp ranged from 0% to 0.07%, remaining within the limit of -5%. Radiation output reproducibility varied between 0.07% and 0.11%, likewise lower than the limit of less than -5%. Reproducibility of exposure time ranged from 0% to 0.07%, lower than the limit of less than -10%. The mAs linearity at 70kVp was 1.44%, lower than the limit of less than -20%. Finally, the CoL at 70kVp was recorded at 0.01, not exceeding the limit of 0.1.

#### 3.2.2. Simulation of X-ray spectra in diagnostic radiography

Figures 2, 3, and 4 illustrate that all five computer codes effectively predict the X-ray spectrum of a general diagnostic radiography machine. There are slight differences in the characterization of K-peaks ( $K_{\alpha 1}$ ,  $K_{\alpha 2}$ ,  $K_{\beta 1}$ ,  $K_{\beta 2}$ ). Among the codes, IPEM Report No. 78 and SpekPy demonstrate strong agreement and clearly distinguish the K-peaks. In contrast, Spektr 3.0 and Xpecgen show superposition of  $K_{\alpha 1}$  and  $K_{\alpha 2}$ ,  $K_{\beta 1}$  and  $K_{\beta 2}$  peaks. The EGSnrc MC shows the “hardest” spectrum of all-over codes. Table 7 highlights minor variations in the energy positions of K-peaks across the codes. These discrepancies can be attributed to the difference in the fitting model and in the electron and bremsstrahlung models used, as detailed in Table 2. Furthermore, the use of different target materials should be considered: IPEM report No.78 and MC EGSnrc use a W/Re target with 10%Re while SpekPy, Xpecgen, and Spectr 3.0 use a pure W target.

#### 3.2.3. Comparisons of the HVL, $E_{mean}$ , and $K_{air}/mAs$ at various tube voltages

Table 4 compares the HVL for various tube voltages of physical experiments and simulated using five computer codes. The percentage differences (Diff, %) varied between 1.16% to 3.71% for 70kVp, 0.64% to 3.61% for 80kVp, and 0.11% to 3.13% for 90kVp. The Diff, % of SpekPy increased while other computer codes decreased with increasing tube voltage. All simulated and physical measurements of HVL for various kVp satisfied the minimum requirements of IEC 60601-1-3. Table 5 compares the  $E_{mean}$  for various tube voltages of physical experiments and simulated using five computer codes. The Diff, % varied between 0.24% to 8.95% for 70kVp, 0.07% to 6.29% for 80kVp, and 0.08% to 7.00% for 90kVp. Table 6 compares the  $K_{air}/mAs$  for various tube voltages of physical experiments and those simulated using five computer codes. The Diff, % varied between 2.60% to 8.12% for 70kVp, 1.70% to 7.90% for 80kVp, and 2.40% to 7.84% for 90kVp.

#### 3.2.4. Assessment of anode heel effect and anode composition in diagnostic radiography

Figure 5 illustrates the anode heel effect at various kVp. Differences in  $K_{air}/mAs$  from -20cm anode side to 20cm cathode side of the central axis with and without aluminium filter are shown in Table 8. It can be seen that the difference in  $K_{air}/mAs$  of the diagnostic radiography

increased by increasing the kVp. When aluminum filters were added, this difference was reduced and produced a uniform distribution of the radiation intensity.

Figure 6 shows the EGSnrc MC simulated spectra for various target compositions at 90kVp. In this study, we present the results of the simulation of the X-ray spectrum with target materials with %W/%Re ratios of 100W/0Re, 95W/05Re, 90W/10Re, 85W/15Re, 80W/20Re, and 70W/30Re. The total fluence over the spectrum was normalized to unity. It is seen that the total fluence is highest at 95%W/5%Re and then gradually decreases with %Re of 10, 15, 30, and 20%. The pure W target had the lowest total fluence. Although the target with 95%W/05%Re had the highest efficiency, the X-ray spectra produced more low-energy photons, which reduced images contrast and increased patient exposure dose.

#### 4. Conclusions

In this study, five computer codes were employed to simulate the X-ray spectrum, and their outputs were compared. The results show that the X-ray spectrum generated by SpekPy is in the best agreement with that of IPEM report No.78. In contrast, Xpecgen, Spektr 3.0, and EGSnrc MC show a significant difference in K-peaks intensity. Specifically, the intensity of K-peaks in IPEM report No.78 and SpekPy are significantly higher than those obtained from Xpecgen, Spektr 3.0, and EGSnrc MC for 80 and 90kVp. The comparative assessment showed that the HVL,  $E_{\text{mean}}$ , and  $K_{\text{air}}/\text{mAs}$  were well-matched between the five codes and physical measurements. The HVL obtained from the simulations satisfied the minimum requirements of IEC 60601-1-3. The anode heel effect and target material composition were also evaluated by using SpekPy and EGSnrc MC codes, respectively. Empirical and semi-empirical codes can offer rapid computation, often under one minute, but are limited in flexibility, as they cannot accommodate arbitrary target/filter materials or complex geometric configurations. In contrast, the MC simulation, though time-consuming, provides more comprehensive data on electron interactions with target/filter combinations of any material composition. This capability is particularly valuable for designing new target materials and optimizing image quality in diagnostic radiography.

❖ **Conflict of Interest:** Authors have no conflict of interest to declare.

#### REFERENCES

- Archer, B. R., & Wagner, L. K. (1988). Determination of diagnostic X-ray spectra with characteristic radiation using attenuation analysis. *Medical Physics*, 15(4), 637-641.
- Ay, M. R., Shahriari, M., Sarkar, S., Adib, M., & Zaidi, H. (2004). Monte Carlo simulation of X-ray spectra in diagnostic radiology and mammography using MCNP4C. *Physics in Medicine and Biology*, 49(21), 4897-4917.
- Bethe, H., (1930). Zur theorie des durchgangs schneller korpuskularstrahlen durch materie. *Ann. Phys.*, 397, 325-400.
- Birch, R., & Marshall, M. (1979). Computation of bremsstrahlung X-ray spectra and comparison with spectra measured with a Ge(Li) detector. *Physics in Medicine and Biology*, 24(3), 505-517.

- Blough, M. M., Waggener, R. G., Payne, W. H., & Terry, J. A. (1998). Calculated mammographic spectra confirmed with attenuation curves for molybdenum, rhodium, and tungsten targets. *Medical Physics*, 25(9), 1605-1612.
- Boone, J. M., & Seibert, J. A. (1997). An accurate method for computer-generating tungsten anode x-ray spectra from 30 to 140 kV. *Medical Physics*, 24(11), 1661-1670.
- Boone, J. M., Fewell, T. R., & Jennings, R. J. (1997). Molybdenum, rhodium, and tungsten anode spectral models using interpolating polynomials with application to mammography. *Medical Physics*, 24(12), 1863-1874.
- Bujila, R., Omar, A., & Poludniowski, G. (2020). A validation of SpekPy: A software toolkit for modelling X-ray tube spectra. *Physica medica : PM : An international journal devoted to the applications of physics to medicine and biology : Official journal of the Italian Association of Biomedical Physics (AIFB)*, 75, 44-54. Advance online publication.
- Fewell, T. R., & Shuping, R. E. (1977). Photon energy distribution of some typical diagnostic X-ray beams. *Medical Physics*, 4(3), 18-197.
- Hernandez, A. M., & Boone, J. M. (2014). Tungsten anode spectral model using interpolating cubic splines: unfiltered x-ray spectra from 20 kV to 640 kV. *Medical Physics*, 41(4), Article 042101.
- Hernández, G., & Fernández, F. (2016). A model of tungsten anode x-ray spectra. *Medical Physics*, 43(8), Article 4655.
- Hyemin, P., Jungmin, K., Jungsu, K., Seong-ok, K., & Young-min, C. (2018). Amendment of the Inspection Standard for Diagnostic Radiation Equipment Applying IEC 60601-1-3: Medical Electrical Equipment – Part 1-3: General Requirements for Basic Safety and Essential Performance – Collateral Standard: Radiation Protection in Diagnostic X-ray Equipment. *Journal of Radiological Science and Technology*, 41(5), 493-504.
- Iles, W. J. (1987). *The computation of Bremsstrahlung X-ray spectra over an energy range 15 keV to 300 keV (NRPB-R--204)*. United Kingdom.
- International Atomic Energy Agency. (2023). *Handbook of basic quality control tests for diagnostic radiology* (No. 47 in Human Health Series). IAEA. ISBN 978-92-0-130322-6
- Kawrakow, I. (2000). *EGSnrc toolkit for Monte Carlo simulation of ionizing radiation transport*. National Research Council Canada.
- Kulkarni, R. N., & Supe, S. J. (1984). Monte Carlo calculations of mammographic X-ray spectra. *Physics in Medicine and Biology*, 29(2), 185-190.
- Math. Graphics. Programming. (2023). <https://www.mathworks.com/products/matlab.html>; [Accessed 18 January 2023].
- MathWorks. (2023). *MATLAB* [Computer software]. <https://www.mathworks.com/products/matlab.html>
- Morrison, G. D. (1998). [Review of the book *Catalogue of Diagnostic X-ray Spectra and Other Data* (IPEM Report 78), by K. Cranley, B. J. Gilmore, G. W. A. Fogarty, & L. Desponds (Eds.)]. *Radiography*, 4(2), 228-229.
- National Institute of Standards and Technology. (2004, July). *X-ray mass attenuation coefficients*. U.S. Department of Commerce. <https://www.nist.gov/pml/x-ray-mass-attenuation-coefficients>
- Ng, K. P., Kwok, C. S., & Tang, F. H. (2000). Monte Carlo simulation of X-ray spectra in mammography. *Physics in Medicine and Biology*, 45(5), 1309-1318.
- Punnoose, J., Xu, J., Sisniega, A., Zbijewski, W., & Siewerdsen, J. H. (2016). Technical Note: Spektr 3.0-A computational tool for x-ray spectrum modeling and analysis. *Medical Physics*, 43(8), Article 4711.
- Rogers, D. W. O., Walters, B. R. B., & Kawrakow, I. (2009). *BEAMnrc users manual* (NRC Report PIRS-0509). National Research Council of Canada.

- Salvat, F., Fernández-Varea, J. M., & Sempau, J. (2011). \*PENELOPE-2008: A code system for Monte Carlo simulation of electron and photon transport\* (NEA/NSC/DOC[2011]5). Nuclear Energy Agency. <https://www.oecd-nea.org/upload/docs/application/pdf/2019-12/penelope2008.pdf>
- Shaw, D., Worrall, M., Baker, C., Charnock, P., Fazakerley, J., Honey, I., Iball, G., Koutaloni, M., Price, M., Renaud, C., Rose, A., & Wood, T. (2020). IPEM Topical Report: An evidence and risk assessment based analysis of the efficacy of quality assurance tests on fluoroscopy units-part II; image quality. *Physics in medicine and biology*, 65(22), Article 225037.
- Taleei, R., & Shahriari, M. (2009). Monte Carlo simulation of X-ray spectra and evaluation of filter effect using MCNP4C and FLUKA code. *Applied radiation and isotopes: including data, instrumentation and methods for use in agriculture, industry and medicine*, 67(2), 266-271.
- Townson, R., Tessier, F., Mainegra, E., & Walters, B. (2020). Getting started with EGSnrc. *Nrc Rep Pirs*, 12, 10-43.
- Tucker, D. M., Barnes, G. T., & Chakraborty, D. P. (1991). Semiempirical model for generating tungsten target x-ray spectra. *Medical Physics*, 18(2), 211-218.
- Tucker, D. M., Barnes, G. T., & Wu, X. Z. (1991). Molybdenum target X-ray spectra: A semiempirical model. *Medical Physics*, 18(3), 402-407.
- Waggener, R. G., Blough, M. M., Terry, J. A., Chen, D., Lee, N. E., Zhang, S., & McDavid, W. D. (1999). X-ray spectra estimation using attenuation measurements from 25 kVp to 18 MV. *Medical Physics*, 26(7), 1269-1278.
- Whiddington, R. (1912). The transmission of cathode rays through matter. *Proceedings of the Royal Society of London. Series A*. 86, 360-370.
- Wolfram Mathematica: Modern technical computing. (2023). Retrieved January 18, 2023 from <https://www.wolfram.com>
- Yagi, H., Kitamura, R., Saruwatari, R., Doi, N., & Yamane, E. (2003). *Nihon Hoshasen Gijutsu Gakkai zasshi*, 59(6), 729-736.

## ĐÁNH GIÁ CÁC MÃ MÁY TÍNH KHÁC NHAU ĐỂ TẠO PHỔ TIA X TRONG X QUANG CHẨN ĐOÁN THƯỜNG QUY

**Bùi Ngọc Huy\*, Phạm Văn Dũng**

*Viện Nghiên cứu Hạt nhân Đà Lạt, Việt Nam*

*\*Tác giả liên hệ: Bùi Ngọc Huy –Email: huyngoc192@yandex.ru*

*Ngày nhận bài: 18-9-2023; ngày nhận bài sửa: 30-10-2023; ngày duyệt đăng: 13-11-2023*

### TÓM TẮT

Nghiên cứu này trình bày kết quả mô phỏng phổ tia X của máy chụp X quang chẩn đoán tổng hợp bằng cách sử dụng mô hình thực nghiệm (Spektr 3.0), mô hình bán thực nghiệm (báo cáo IPEM số 78, SpekPy và Xpecgen) và phương pháp Monte Carlo (EGSnrc). Máy X-quang chẩn đoán thường quy được tiến hành kiểm định chất lượng. Bề dày hấp thụ một nửa (HVL), năng lượng trung bình ( $E_{mean}$ ) và Air kerma trên mỗi mAs ( $K_{air}/mAs$ ) đã được đo thực nghiệm ở các điện áp đỉnh khác nhau và được so sánh với các giá trị thu được từ năm mã máy tính. Hiệu ứng gót chân và thành phần vật liệu bia anode cũng được nghiên cứu. Báo cáo IPEM số 78 được sử dụng làm tài liệu tham khảo để so sánh với các mã máy tính khác. Đánh giá so sánh cho thấy HVL,  $E_{mean}$  và  $K_{air}/mAs$  rất phù hợp giữa năm mã và phép đo vật lý trong phạm vi năng lượng X quang chẩn đoán. Phương pháp Monte Carlo là một công cụ tính toán phức tạp, chính xác, có thể mô tả phổ tia X của các thành phần vật liệu bia mới được phát triển, cấu hình hình học phức tạp và sự đóng góp của các hạt thứ cấp, điều mà hầu hết các mô hình thực nghiệm và bán thực nghiệm hiện không thể thực hiện chính xác.

**Từ khóa:** mô phỏng EGSnrc; bề dày hấp thụ một nửa; Monte Carlo; phổ tia X; X-quang